Effects of Halides and Bicarbonate on Chloride Transport in Human Red Blood Cells

MADS DALMARK

From the Department of Biophysics, University of Copenhagen, Copenhagen, Denmark

ABSTRACT Chloride self-exchange was determined by measuring the rate of ^{36}Cl efflux from human red blood cells at pH 7.2 (0°C) in the presence of fluoride, bromide, iodide, and bicarbonate. The chloride concentration was varied between 10–400 mM and the concentration of other halides and bicarbonate between 10–300 mM. Chloride equilibrium flux showed saturation kinetics. The half-saturation constant increased and the maximum flux decreased in the presence of halides and bicarbonate: the inhibition kinetics were both competitive and noncompetitive. The competitive and the noncompetitive effects increased proportionately in the sequence: fluoride < bromide < iodide. The inhibitory action of bicarbonate was predominantly competitive. The noncompetitive effect of chloride (chloride self-inhibition) on chloride transport was less dominant at high inhibitor concentrations. Similarly, the noncompetitive action of the inhibitors was less dominant at high chloride concentrations. The results can be described by a carrier model with two anion binding sites: a transport site, and a second site which modifies the maximum transport rate. Binding to both types of sites increases proportionately in the sequence: fluoride < chloride < bromide < iodide.

INTRODUCTION

It appears from recent investigations that chloride equilibrium transport in human red blood cells takes place by facilitated diffusion (Wieth, 1972; Gunn et al., 1973; Dalmark, 1975 *b*). Other halides and bicarbonate reduce chloride self-exchange (Dalmark and Wieth, 1972). This paper presents kinetic evidence that the influences of fluoride, bromide, iodide, and bicarbonate are both competitive and noncompetitive. The inhibitory action of chloride on its own transport is explained by analogy with the noncompetitive effects of other halides.

METHODS AND CALCULATIONS

All experiments were performed by determining the rate of ^{36}Cl efflux from human red cells. Conditions were arranged so that there was no net flux of chloride across the cell membrane, i.e. the net loss of radioactive chloride was balanced by an equal uptake of nonradioactive chloride.

Freshly drawn, heparinized human blood was titrated with CO_2 to pH 7.2 (0°C). The CO_2/bicarbonate was removed from the cells by four washes with a solution containing 150 mM KCl, 1 mM NaCl, 27 mM sucrose. After removal of CO_2/bicarbonate the system was buffered by the intracellular buffers, mainly hemoglobin.

The concentration of salts in cells was altered by the nystatin technique as previously described (Cass and Dalmark, 1973; Dalmark, 1975 *a*). The electrolyte solutions employed

for the preparation of cells, for the incubation of cells with ^{36}Cl, and for the efflux experiments had the following composition (mM): 0-300 X, 5-400 KCl, 1 NaCl, 27 sucrose. X indicates KF, KBr, KI, or $KHCO_3$. After removal of nystatin from the cells the pH was adjusted to 7.2 (0°C). In the presence of $KHCO_3$ the system was buffered by CO_2.

Labeling of cells with ^{36}Cl, isolation of labeled cells, determination of radioactivity in cells and medium, and the technique of flux measurements have previously been described (Dalmark and Wieth, 1972): the ^{36}Cl efflux from labeled cells to medium was followed by serially isolating cell-free medium by rapid filtration from the cell suspension (hematocrit < 0.01 [vol/vol]) at pH 7.2 (0°C).

Calculations

The exchange kinetics of chloride was well described in all experiments by a closed two-compartment model with constant volumes (Fig. 1 *a* and *b*). The equation describing the time dependence of the specific activity in the medium is

$$a_t = a_\infty(1 - e^{-bt}), \tag{1}$$

where a_t is the specific activity at time t, a_∞ the specific activity in both phases at isotopic equilibrium, and the exponent b is equal to the sum of the rate coefficients for isotope efflux (k^o) and influx (k^i). The exponent b approaches k^o, when the hematocrit is low. The hematocrit was below 0.01 (vol/vol) in the present experiments, and k^o, therefore, constituted more than 98% of the value of b. The rate coefficient of chloride exchange was calculated from the relation between $\ln(1 - a_t/a_\infty)$ and the time, t, by a least square regression analysis. The slope of the graph was assumed to be equal to $-k^o$.

The chloride equilibrium flux (efflux = influx) was calculated from the equation:

$$M^{Cl}(\text{mmol Cl}/3 \times 10^{13}\ \text{cells}\cdot\text{min}) = k^o \times V \times (Cl)_c \times F, \tag{2}$$

where k^o is the rate coefficient of tracer efflux (min^{-1}), V is the cellular water content (kilogram water per kilogram solids), $(Cl)_c$ is the cellular chloride concentration (millimoles per kilogram cell water), and F has the dimension kilogram cell solids/3×10^{13} cells (Dalmark, 1975 *a*). The 3×10^{13} cells have a surface area of 4,890 m^2 (Ponder, 1948) and contain 1 kg cell solids at an ionic strength of 0.15 (Funder and Wieth, 1966). The value of F was calculated from the molecular weights and the cellular concentrations of the inhibiting ions.

RESULTS

The results will be described in three sections. The first two contain, respectively, experimental data and a kinetic analysis from studies in which chloride equilibrium flux was measured in cells pretreated with nystatin, so that the ionic strength of the intra- and extracellular fluids could be varied without affecting cell volume. The third section describes experiments done at normal ionic strength, with no preceding nystatin exposure. It will be shown that pretreatment of cells with nystatin does not alter the inhibition kinetics.

All experiments were performed at pH 7.2 and 0°C. It was previously shown (Dalmark, 1975 *a*) that under these conditions the chloride concentrations in cell and medium water are equal, provided the ionic strength is greater than 0.05. This greatly simplifies the analysis, because one can compute the kinetics of chloride flux without the complicating feature of a difference in chloride concentration on either side of the membrane. Furthermore, it is generally believed (*a*)

that the hydroxyl ion distribution is close to the chloride distribution across the cell membrane (reviewed by Dalmark, 1975 *b*), and (*b*) that the electrical membrane potential difference is equal to the chloride equilibrium potential. If so, the experiments were carried out under conditions where (*a*) the chloride and proton concentrations were equal in cell water and medium, and (*b*) the membrane potential difference was zero.

In comparing the present data with data previously published of chloride equilibrium flux in the absence of other anions (Dalmark, 1975 *b*), it is necessary to take into account the change in chloride distribution ratio which occurs at low ionic strengths. A method for making this correction has been described (Dalmark, 1975 *b*), and has been used in Fig. 8 to give values of uninhibited chloride flux at a chloride distribution ratio of unity.

Influence of Halides and Bicarbonate on Chloride Flux (Varying Ionic Strength)

Fig. 1 shows the time-course of ^{36}Cl efflux from labeled cells in solutions at various ionic strengths. At a constant chloride of 21 mM the half time of isotope movement rose from 10 to 87 as bromide (Br) was increased from 40 to 300 mM (Fig. 1 *a*). Similarly, with Br constant at 40 mM, an eightfold increase in the halftime for isotope flux was observed on raising the chloride from 10 to 400 mM (Fig. 1 *b*). The effects of fluoride (F), iodide (I), and bicarbonate (HCO_3) on ^{36}Cl efflux were qualitatively similar to those in Fig. 1. Calculation of flux values from these data (cf. *Methods* section) gave graphs such as Fig. 2. In all cases the chloride flux showed saturation kinetics.

Inspection of Fig. 2 shows that the inhibitory actions of the various halides on

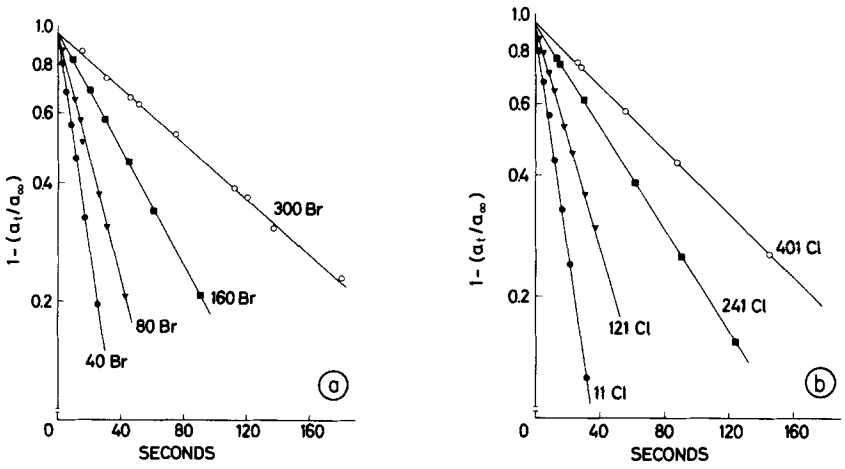

FIGURE 1. The rate of ^{36}Cl efflux from radioactively labeled human red blood cells under conditions with no chloride net flux (0°C, pH 7.2). Fig. 1 *a* shows the effect of different Br concentrations (● 40 mM, ▼ 80 mM, ■ 160 mM, ○ 300 mM) on the rate at a constant Cl concentration of 21 mM. Fig. 1 *b* shows the effect of different Cl concentrations (● 11 mM, ▼ 121 mM, ■ 241 mM, ○ 401 mM) on the rate at a constant Br concentration of 40 mM.

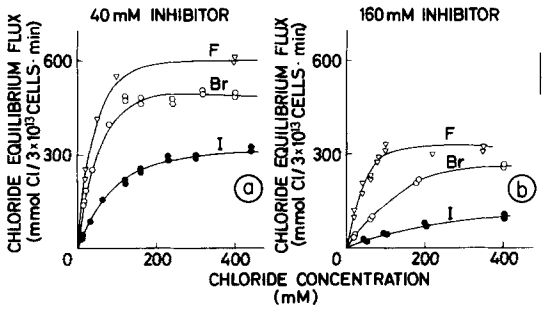

FIGURE 2. The dependence of chloride equilibrium flux (0°C, pH 7.2) on chloride concentration in the presence of F(▽), Br(○), and I(●) at concentration of 40 mM (Fig. 2 *a*) and 160 mM (Fig. 2 *b*). The curves were drawn by eye.

chloride transport were exerted on both the maximum rate and the half-saturation value ($K^1/_2$), indicating both competitive and noncompetitive effects which will be quantitated in the following section. This mixed inhibition was observed at all inhibitor concentrations tested over a range from 40 to 300 mM, as exemplified by Br in Fig. 3. The degree of both competitive and noncompetitive inhibition increased in the sequence F < Br < I. Bicarbonate showed mixed inhibitory effects qualitatively similar to those of the halides, as shown in Fig. 4 *a*. The inhibitory action of the various anions was not an effect of the ionic strength in the bulk phases on both sides of the cell membrane since the chloride transport was markedly different at the same temperature, pH, chloride, and inhibitor concentration (Fig. 2).

Kinetic Analysis of the Data (Varying Ionic Strength)

Figs. 4 *b* and 5 show Woolf-Hofstee plots of the bicarbonate and halide data (Hofstee, 1959). In such graphs a linear relationship indicates simple Michaelis-Menten kinetics with $K^1/_2$ equal to the reciprocal slope and the maximum rate given by the intercept with the abscissa.

At low inhibitor concentration (~40 mM) all experiments showed linear graphs only at low transport values. At high flux rates, corresponding to high chloride concentrations, the graphs bend downwards towards the abscissa. This deviation from Michaelis-Menten kinetics has also been observed at high chloride concentrations when chloride was the only anion in the system and was termed "chloride self-inhibition" (Dalmark, 1975 *b*). This self-inhibition appears to be analogous to the noncompetitive effects of F, Br, I, and HCO_3 on chloride transport.

As levels of HCO_3 (Fig. 4 *b*) and I (Fig. 5 *b*) were increased, the Woolf-Hofstee plots became increasingly linear in the range of chloride concentration 0-400 mM. A similar effect was noted with F and Br. These findings indicate that at high inhibitor concentrations chloride self-inhibition is reduced.

The *linear* portions of the Woolf-Hofstee plots were used to compute values of $K^1/_2$ and (maximum chloride transport)$^{-1}$. Both these functions were found to be linearly related to inhibitor concentration (Fig. 6 *a* and *b*). The effectiveness of the various anions as inhibitors of chloride transport increases in the sequence F

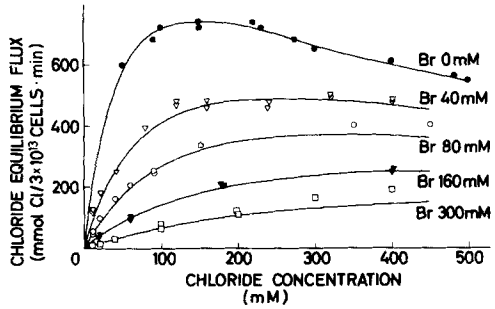

FIGURE 3. Comparison between calculated (−) and measured (symbols) chloride equilibrium flux (0°C, pH 7.2) in the presence of bromide (mM): 0 Br, ●; 40 Br, ▽; 80 Br, ○; 160 Br, ▼; 300 Br, □. The calculated flux was determined from the equation for the model (cf. Appendix, Eq. 2 *a*), with the following values inserted for the various constants (cf. Discussion and Table I): P_{4Cl} (T) 1,550 mmol Cl/3 × 10^{13} cells·min, K_{Cl} 67 mM, K_{ClCl} 335 mM, K_{Br} 32 mM, K_{BrBr} 160 mM.

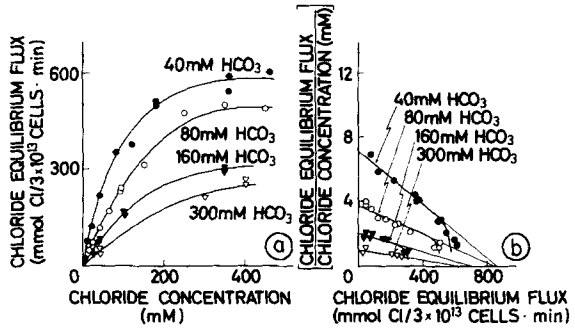

FIGURE 4. Fig. 4 *a* shows the dependence of chloride equilibrium flux (0°C, pH 7.2) on chloride concentration in the presence of different HCO_3 concentrations (● 40 mM, ○ 80 mM, ▼ 160 mM, ▽ 300 mM). Fig. 4 *b* shows the data of Fig. 4 *a* plotted as described by Woolf-Hofstee (Hofstee, 1959).

< Br < I. Extrapolation of all graphs to zero inhibitor concentration gave identical intercepts with the oridinate at reciprocal theoretical maximum chloride transport (Fig. 6 *a*) (900 mmol/3 × 10^{13} cells·min)$^{-1}$, and at theoretical $K^1/_2$ (Fig. 6 *b*) 33 mM. These values agree well with previously published figures for chloride transport in red cells at concentrations below 170 mM when chloride was the only anion in the system (Dalmark, 1975 *b*).

The graphs in Fig. 6 *a* and *b* are described by the empirical equations: $(M(\text{max})(\text{mmol Cl/3} \times 10^{13} \text{ cells·min}))^{-1} = (1/900)\,(1 + (R)/K_{RR})$, and $(K^1/_2)$ (mM) $= 33\,(1 + (R)/K_R)$, where (R) (mM) is the inhibitor concentration and K_R and K_{RR} (mM) are constants which depend on the species of inhibitor. Table I shows that there is a proportionate decrease in the value of both K_R and K_{RR} as one goes from F to Br to I. The ratio, K_{RR}/K_R, is of the same magnitude for the three halides. Bicarbonate shows a much higher ratio of K_{RR} to K_R, signifying that, compared to halides, bicarbonate inhibition of chloride transport is dominated by competitive effects.

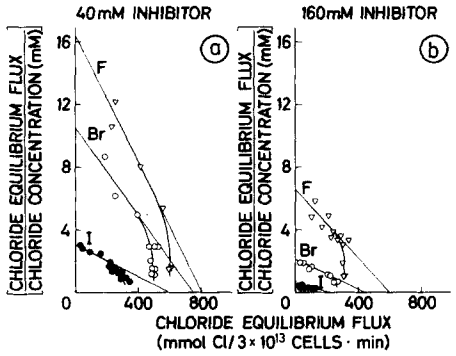

FIGURE 5. The data of Fig. 2 *a* and *b* plotted as described by Woolf-Hofstee (Hofstee, 1959). The graphs indicate the curves drawn by eye in Fig. 2 *a* and *b*, and measured values are indicated by ▽ (F), ○ (Br), and ● (I).

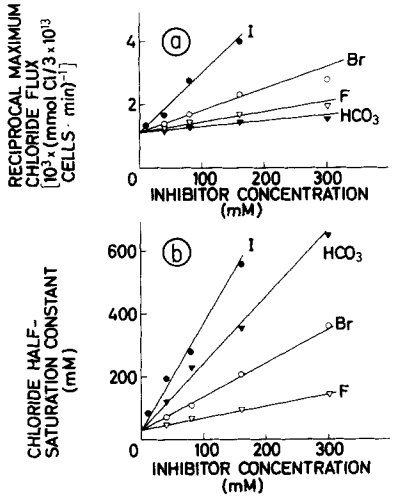

FIGURE 6. The dependence of the reciprocal maximum chloride transport (Fig. 6 *a*) and the half-saturation constant ($K^1/_2$) (Fig. 6 *b*) on the concentration of F(▽), Br(○), I(●), and HCO_3(▼) at 0°C (pH 7.2). The maximum chloride transport and the $K^1/_2$ were determined from the linear portions of graphs in Woolf-Hofstee plots (cf. Figs. 5 *a* and *b*, 4 *b*).

Fig. 7 shows reciprocal chloride flux as a function of inhibitor concentration at various constant chloride concentrations, following the procedure of Dixon (Dixon, 1953). Such plots are helpful in characterizing pure cases of competitive or noncompetitive inhibition. The method is misleading when both types of inhibition are present and only a small concentration range is investigated. At low concentrations of Br and I, straight lines intersecting above the abscissa can be drawn, suggesting pure competitive effects. But at higher inhibitor concentrations the plots deviate increasingly from linearity when the chloride concentration is low (~20 mM). The fluoride points, which resemble a classic instance of

TABLE I

INHIBITOR CONSTANTS FOR COMPETITIVE (K_R) AND NONCOMPETITIVE (K_{RR}) INHIBITION OF CHLORIDE EQUILIBRIUM FLUX BY HALIDES AND BICARBONATE (0°C, pH 7.2)

Inhibitor	K_R	K_{RR}	K_{RR}/K_R
	mM	*mM*	
Fluoride	88	337	4
Bromide	32	160	5
Iodide	10	60	6
Bicarbonate	16	585	37

The inhibitor constants were calculated from the slopes of the linear graphs of reciprocal maximum chloride transport and half-saturation constant of chloride transport vs. inhibitor concentration (cf. Fig. 6 *a* and *b*).

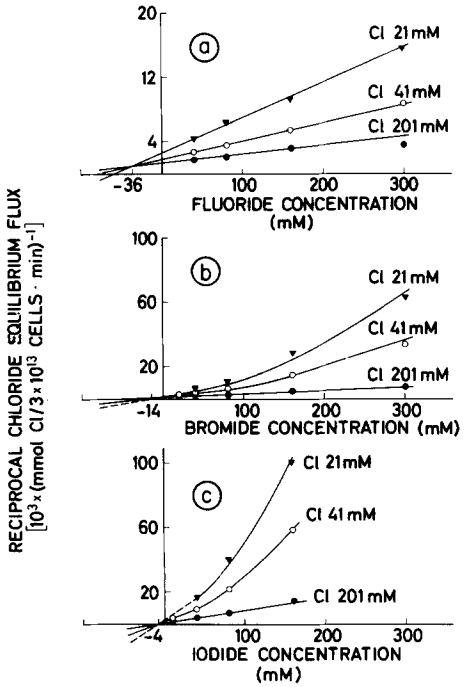

FIGURE 7. The dependence of the reciprocal chloride equilibrium flux (0°C, pH 7.2) on the concentration of F (Fig. 7 *a*), Br (Fig. 7 *b*), and I (Fig. 7 *c*) at three different Cl concentrations (▼ 21 mM, ○ 41 mM, ● 201 mM) plotted as described by Dixon (1953). The intersection points of the graphs left of the origin indicate *apparent* competitive inhibitor constants (mM): 36(F), 14(Br), 4 (I).

competitive inhibition by the Dixon plot criteria, would presumably show deviations from linearity at higher F concentrations. Thus, the values obtained from the intersection points to the left of the origin must be regarded as *apparent* competitive inhibitor constants. As will be shown, these numbers agree well with

constants derived from studies at normal ionic strength. Similar Dixon plots for bicarbonate (not shown) gave linear graphs with concentrations of inhibitor up to 300 mM. The apparent inhibitor constant for bicarbonate was 10 mM, agreeing with the value of 6 mM reported by Gunn et al. (1973).

At low chloride concentrations (~20 mM), the Dixon plots are nonlinear, suggesting that the noncompetitive effects of Br and I were dominant. At high chloride concentrations (~200 mM) the noncompetitive action of the inhibitors is greatly diminished, as indicated by the linearity of the Dixon plots. The linearization of the Woolf-Hofstee plots at high inhibitor concentrations and of the Dixon plots at high chloride concentrations suggests that the kinetics of chloride transport are dominated by noncompetitive effects, either of the various inhibitors or of chloride itself, depending on their relative concentrations. The noncompetitive inhibitory actions of bicarbonate and F were less than those of Br and I (Figs. 5, 4 *b*, and Table I), and the Dixon plots were linear in the concentration range employed.

Inhibition Experiments at Normal Ionic Strength

In the following experiments, halides and bicarbonate were substituted for chloride, and the chloride equilibrium flux was measured at pH 7.2 (Fig. 8). The cells were not exposed to nystatin. The dashed line shows chloride flux in

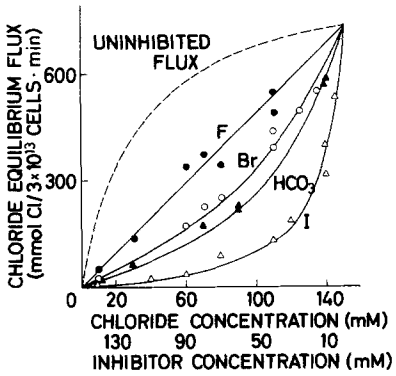

FIGURE 8. The dependence of chloride equilibrium (0°C, pH 7.2) on chloride concentration when F(●), Br(○), I(△), and HCO_3(▲) were substituted for chloride. The sum of chloride and inhibitor was 150 mM. The dashed graph shows the uninhibited chloride transport, as calculated from the equation:

$$M^{Cl} = 900\ [1 + 33/(Cl)]^{-1}\ (\text{mmol Cl}/3 \times 10^{13}\ \text{cells}\cdot\text{min}),$$

where (Cl) indicates chloride concentration in cells and medium. The solid lines indicate the best fits of measured values to pure competitive inhibition kinetics, as calculated from the equation:

$$M_R^{Cl} = 900\ [1 + 33(1 + (R)/K'_R)/(Cl)]^{-1}\ (\text{mmol Cl}/3 \times 10^{13}\ \text{cells}\cdot\text{min}),$$

where (R) is the concentration and K'_R (mM) the apparent competitive inhibitor constant of the ion species R.

absence of other anions calculated for a situation where the chloride distribution ratio between cell water and medium is unity. This was done by inserting the extrapolated values for $K^1/_2$ and maximum flux from Fig. 6 at zero inhibitor concentration into a simple Michaelis-Menten equation. It is necessary to construct such a graph for the case in which no anion substitution is made: as explained above, the cell/medium chloride ratio is not unity at low ionic strength.

The solid lines in Fig. 8 respresent the best fits of the experimental data to an equation for pure competitive inhibition kinetics (cf. legend to Fig. 8). The inhibitor constants for F, Br, I, and HCO_3 were 33, 12, 2, and 8 mM, respectively. These values are virtually identical with those obtained from Dixon plots at low inhibitor concentrations in the nystatin-pretreated cells (Fig. 7). This justifies the statement that the preceding nystatin treatment did not alter the inhibition kinetics.

Thus, the hazards of drawing conclusions from data obtained in a limited concentration range are demonstrated: For while substitution experiments at normal ionic strength give the impression of pure competitive inhibition, the Dixon plots for nystatin-treated cells over a wider ionic strength range demonstrate a more complex inhibition mechanism. This is also shown in the Woolf-Hofstee plots.

DISCUSSION

When the kinetics of chloride transport are studied in the absence of other anions, an anomalous saturation curve is obtained which passes through a maximum (Cass and Dalmark, 1973). The information presented here on halide and bicarbonate effects makes it possible to account for the shape of this graph by regarding chloride as a noncompetitive inhibitor of its own transport.

The results can be fitted to the model for carrier-mediated transport previously proposed (Wieth, 1972; Gunn, 1972). The present formulation envisions that chloride transport is carried out by a mechanism involving two types of binding sites, transport sites and modifier sites (cf. Appendix). Anions which combine with transport sites are carried through the membrane. Anions which combine with modifier sites reduce the total number of transportable carriers and, therefore, the maximum flux rate. Competition among different anion species for the transport sites is reflected by an increasing half-saturation constant, while competition at the modifier sites influences the maximum transport rate. Halides and bicarbonate represent anions which combine with both types of binding sites. The general equation for the model, derived in the Appendix, states that

$$M_R^{Cl} = P_{ACl}(T)[1 + (Cl)/K_{ClCl} + (R)/K_{RR}]^{-1}[1 + K_{Cl}(1 + (R)/K_R)/(Cl)]^{-1},$$

where M_R^{Cl} is the chloride equilibrium flux in the presence of the inhibitor R. K_{ClCl} and K_{RR} are the dissociation constants (mM) at the modifier sites, and K_{Cl} and K_R are the dissociation constants (mM) at the transport sites. P_{ACl} (T) is the theoretical maximum rate of chloride transport (mmol/3 $\times$ 10^{13} cells·min). This

would be the maximum chloride flux if there were no noncompetitive influences due to interaction of chloride with the modifier sites on the carriers.

To describe the shape of the chloride transport saturation curve in the absence of other anions it is necessary to calculate values for the constants $P_{ACl}(T)$, K_{Cl}, and K_{ClCl}. This can be done (cf. Appendix) from the experimentally derived information (Dalmark, 1975 *b*) that (*a*) a maximum chloride flux of 740 mmol/3 × 10^{13} cells·min *is observed* at an optimum chloride concentration of 150 mM, and that (*b*) a chloride flux of (740/2)mmol/3 × 10^{13} cells·min *is observed* at 23 mM when chloride concentration on both sides of the membrane is equal. By analogy with the other halides (Table I) one selects the solutions of the equations given in the Appendix which give K_{Cl} smaller than K_{ClCl}. The results of these calculations give values for $P_{ACl}(T)$ of 1,550 mmol/3 × 10^{13} cells·min, for K_{Cl} of 67 mM, and for K_{ClCl} of 335 mM. Comparing the calculated dissociation constants with the data in Table I, it is notable that the value for K_{Cl} falls within the sequence F < Cl < Br < I. Furthermore, the ratio K_{ClCl}/K_{Cl} is the same as K_{RR}/K_R for the other halides.

When the halides are arranged according to increasing size of the unhydrated anions, viz., F < Cl < Br < I, certain relationships of the sequence to the transport data are clear: As one goes from smaller to larger ions the affinity for both transport and modifier sites (reflected by diminishing values for K_R and K_{RR}) is increased. This accords with previous data on the degree of binding of Cl, Br, and I to cellular constituents (Dalmark and Wieth, 1972). On the other hand, the maximum transport rate decreases with increasing ionic size. The meaning of these relationships for the nature of the *transport process* is not clear, however, because of quantitative considerations: One can compute from the model a value for maximum iodide flux (in the absence of other anions), assuming that (*a*) the total number of carriers (T) and the rate constant for the loaded carrier (P_{AI}) are the same as for chloride and (*b*) that the difference between the transport of the two ion species is due solely to the different binding constants. This calculation predicts that iodide should be transported at half the rate of chloride, while the measured maximum iodide flux (0°C) is 1/260 that of chloride (Dalmark and Wieth, 1972). Thus, the slower transport of larger ions is not explained simply on the basis that they are more tightly bound.

Substituting these values in the model equation, the curves shown in Fig. 3 were generated, showing chloride flux both in the absence of other anions and in the presence of various concentrations of bromide. The correspondence with experimental points indicates that the model equation provides a description of the relationships. It must be pointed out, however, that a number of the other models, including one in which noncompetitive inhibition is viewed as influencing the rate of movement of loaded carrier through the membrane, can give rise to similar equations which fit the experimental data equally well.

The present study offers no explanation for the observation of Wood and Passow (1973) that the rate of iodide self-exchange in red cell ghosts is accelerated by chloride and fluoride. All effects of fluoride on chloride transport were inhibitory and could be interpreted as due to interactions with transport sites and modifier sites of the carrier model.

APPENDIX

An Anion Transport Model

This scheme postulates that the human red cell membrane contains mobile components (carriers) which can bind anions and transport them in either direction between cell water and medium. Each carrier has two qualitatively distinctive anion binding sites, one for transport and the other for "modification." A carrier can only move across the membrane when an anion is bound to its transport site and its modifier site is unoccupied. Unloaded carriers, and carriers with anions bound to their modifier sites cannot be translocated but exist in equilibrium with free anions and movable carrier-anion complexes at either surface of the anion barrier. The rate of anion transport is determined not by the interaction between anions and carriers but rather by the mobility of the loaded carrier within the membrane.

In the following scheme A represents the unloaded carrier. Cl and R indicate chloride and an inhibitor anion which, when combined with the modifier site are written to the left of A (ClA, RA) and when bound to the transport site are written to the right of A (ACl, AR). The latter two species, according to the postulates, are the only ones which can be translocated. The various equilibria and the dissociation constants for binding of anions to the transport site (K_{Cl}, K_R) and modifier site (K_{ClCl}, K_{RR}) are diagrammed as follows:

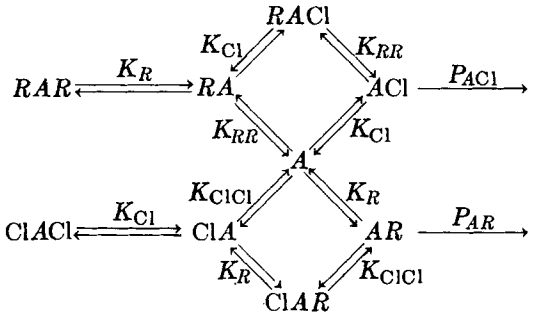

where P_{ACl} and P_{AR} are constants (time^{-1}) for the movement of loaded carrier through the membrane.

Assuming a finite number, (T), of carrier molecules in the membrane, it follows that

$$\begin{aligned}(T) &= (A) + (ACl) + (ClA) + (ClACl) + (RACl) + (AR) + (RA) + (RAR) + (ClAR) \\ &= (ACl)[1 + (Cl)/K_{ClCl} + (R)/K_{RR}][1 + K_{Cl}(1 + (R)/K_R)/(Cl)].\end{aligned} \tag{1 a}$$

The chloride equilibrium flux, M_R^{Cl} is the product of the rate constant P_{ACl} and the number of transportable carrier-chloride complexes (ACl) at the membrane surface:

$$\begin{aligned}M_R^{Cl} &= P_{ACl}(ACl) = \\ &= P_{ACl}(T)[1 + (Cl)/K_{ClCl} + (R)/K_{RR}]^{-1}[1 + K_{Cl}(1 + (R)/K_R)/(Cl)]^{-1}.\end{aligned} \tag{2 a}$$

The chloride equilibrium flux at zero inhibitor concentration is:

$$M^{Cl} = P_{ACl}(T)[1 + (Cl)/K_{ClCl}]^{-1}[1 + K_{Cl}/(Cl)]^{-1}. \tag{3 a}$$

The constants ($P_{ACl}(T)$, K_{Cl}, and K_{ClCl}) of this equation are obtained when the values of the following three expressions are known from experiments: (a) The chloride concentration, $(Cl)_{opt}$, at which maximum chloride flux is observed

$$dM^{Cl}/d(Cl) = 0$$

at

$$(Cl)_{opt} = [K_{Cl}K_{ClCl}]^{1/2}. \quad (4\ a)$$

(*b*) The observed maximum chloride flux, $M^{Cl}(max)_{obs}$,

$$M^{Cl}(max)_{obs} = P_{ACl}(T)[1 + (Cl)_{opt}/K_{ClCl}]^{-1}[1 + K_{Cl}/(Cl)_{opt}]^{-1}. \quad (5\ a)$$

(*c*) The chloride concentration, ($K^1/_2$), at which the chloride flux is half the observed maximum flux

$$^1/_2M^{Cl}(max)_{obs} = P_{ACl}(T)[1 + (K^1/_2)/K_{ClCl}]^{-1}[1 + K_{Cl}/(K^1/_2)]^{-1}. \quad (6\ a)$$

I am glad to express my indebtedness to Mrs. Birgitte Olsen for her valued technical assistance and to Dr. John C. Parker for his comments and suggestions during preparation of the manuscript.

Received for publication 16 May 1975.

REFERENCES

CASS, A., and M. DALMARK. 1973. Equilibrium dialysis of ions in nystatin-treated red cells. *Nat. New Biol.* **244**:47.

DALMARK, M. 1975 *a*. Chloride and water distribution in human red cells. *J. Physiol.* (*Lond.*). **250**:65.

DALMARK, M. 1975 *b*. Chloride transport in human red cells. *J. Physiol.* (*Lond.*). **250**:39.

DALMARK, M., and J. O. WIETH. 1972. Temperature dependence of chloride, bromide, iodide, thiocyanate and salicylate transport in human red cells. *J. Physiol.* (*Lond.*). **224**:583.

DIXON, M. 1953. The determination of enzyme inhibitor constants. *Biochem. J.* **55**:170.

FUNDER, J., and J. O. WIETH. 1966. Potassium, sodium, and water in normal human red blood cells. *Scand. J. Clin. Lab. Invest.* **18**:167.

GUNN, R. B. 1972. A titratable carrier model for both mono- and di-valent anion transport in human red blood cells. *In* Oxygen Affinity of Hemoglobin and Red Cell Acid-Base Status. M. Rørth and P. Astrup, editors. Munksgaard, Copenhagen. 823.

GUNN, R. B., M. Dalmark, D. C. TOSTESON, and J. O. WIETH. 1973. Characteristics of chloride transport in human red cells. *J. Gen. Physiol.* **61**:185.

HOFSTEE, B. H. J. 1959. Non-inverted versus inverted plots in enzyme kinetics. *Nature* (*Lond.*). **184**:1296.

PONDER, E. 1948. Hemolysis and Related Phenomena. Grune and Stratton, New York. 24. 1st edition.

WIETH, J. O. 1972. The selective ionic permeability of the red cell membrane. *In* Oxygen Affinity of Hemoglobin and Red Cell Acid-Base Status. M. Rørth and P. Astrup, editors. Munksgaard, Copenhagen. 265.

WOOD, Ph.G., and H. PASSOW. 1973. Some remarks on the current concepts of the mechanism of anion permeability. *In* Proceedings of Symposium on Drugs and Transport. B. A. Callingham, editor. MacMillans, London.